

Large area avalanche photodiode detector array upgrade for a ruby-laser Thomson scattering system

T. M. Biewer,^{a)} D. J. Den Hartog, and D. J. Holly
Department of Physics, University of Wisconsin-Madison, Madison, Wisconsin 53706

M. R. Stoneking
Physics Department, Lawrence University, Appleton, Wisconsin 54912

(Presented on 8 July 2002)

A low-cost upgrade has been implemented on the Madison Symmetric Torus (MST) ruby-laser Thomson scattering (TS) system to increase spectral coverage and substantially improve the signal-to-noise ratio (SNR). The spectral resolution has been increased from five channels on the long-wavelength side to an 11-channel system, which covers both sides of the laser line. Coverage on both sides of the spectrum allows for more accurate detection of subtle changes in the distribution function, particularly relativistic spectral shifts of high-temperature plasmas during auxiliary current drive. The previous microchannel plate (MCP) detector was replaced with an array of modular large area avalanche photodiode detectors, which have approximately 16 times the quantum efficiency of the MCP detector. Scattered light collection has also been upgraded, allowing the radial viewing location of the TS system to be easily changed between plasma discharges. Improved SNR and upgraded light collection hardware in the Thomson scattering system have facilitated first-time measurements of the evolution of the electron temperature profile in the MST under a variety of discharge conditions, leading to increased understanding of the underlying dynamics of reversed-field pinch plasmas. © 2003 American Institute of Physics.

[DOI: 10.1063/1.1532761]

I. INTRODUCTION

The Madison Symmetric Torus (MST) Thomson scattering (TS) ruby-laser system is relatively robust, and has generated useful data for over 15 years.¹⁻³ The system consists of a JK Lumonics PDS1 ruby-laser head, collection optics, a Jarrell-Ash MonoSpec-27 (Model 82-499) spectrometer, and avalanche photodiode detectors. Over time, the system has evolved through minor and major technological upgrades, but the laser itself has remained the same. It is a single-pulse-per-plasma-shot unit, limited by the time it takes to pump the flashlamps and dissipate the excess heat. It can be operated in “double pulse mode,” however less than half the energy of a single pulse is released in either of the two pulses. Because the system historically has operated on the verge of signal-to-noise practicality, double pulsing the laser has not been an option. To improve the reliability of measurements, multiple shots are usually ensembled together. Prior to the upgrades discussed here, measuring the electron temperature at differing radial locations had only been done in a limited sense.⁴

Hardware upgrades have improved the performance of the ruby TS system. A significant improvement came in 1997 with the addition of a movable fiber optic bundle, which defines the entrance aperture of the light gathering system.⁵ This upgrade made it possible to change viewing geometries between shots, and opened the possibility of measuring temperature profiles (with ensembling) in the matter of a few

days. The capability of the system was further improved in 1998 by the addition of an alternate laser beam line. This doubled the number of viewing locations of the MST Thomson scattering system and expanded the radial range of coverage nearly to the plasma edge. Even with this improved flexibility of the system, it was still severely hampered by low light levels and an unacceptable signal-to-noise ratio (SNR) in the edge region. In 2000 a major upgrade in the light detection system was implemented, greatly improving the light collection efficiency. With this upgrade from the five-channel microchannel plate (MCP) detector to the 11-channel large area-avalanche photodiode detector (LA-APD) array, it became possible to make statistically significant, single shot temperature measurements. The time required to measure a temperature profile was reduced from days to hours, while the resolution of that measurement was increased by a factor of 3. The operating range of the MST has also expanded, reaching record high electron temperatures for the reversed field pinch.⁶ With electron temperatures in excess of 1 keV, relativistic corrections to the electron distribution function become significant, and are measured with the upgraded detector setup.

II. LIGHT COLLECTION SYSTEM

The entire laser system is mounted to a movable cart, which is positioned in close proximity to the MST as shown in Fig. 1.⁷ Once in position, the cart can be raised off its casters to prevent unwanted movement. The laser beam path is mated to the MST through an extension of the vacuum. There are two paths the laser can alternately follow. From the

^{a)}Electronic mail: tbiewer@pppl.gov

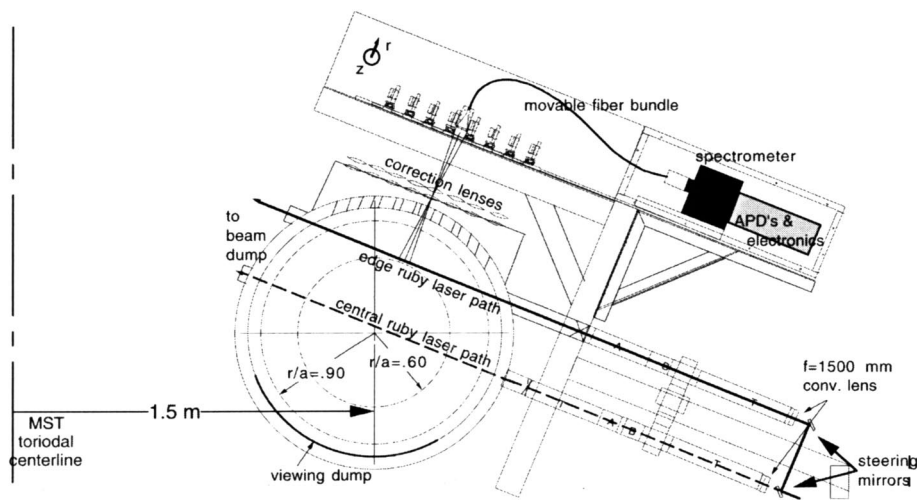


FIG. 1. Side view of the ruby-laser Thomson scattering system at 90° toroidal of the Madison Symmetric Torus. To operate in central laser path mode, the lower steering mirror is removed along with the movable correction lenses.

laser head the beam is turned 157.5° by reflection in a vertical plane from a turning mirror. This angle is set by the poloidal MST box port, which holds the collection optics at an angle of 22.5° . The air-to-vacuum interface is a lens with a focal length of 1500 mm. This lens is at the end of a long pipe, which has both a bellows for mechanical isolation and a delrin segment for electrical insulation. These pipes are supported from the laser-head platform and weakly from a VAT valve at the entrance of the MST vacuum vessel. After passing through the lens, the beam converges to a maximum energy density near the geometrical center of the MST vacuum vessel. On the opposite side of where the beam enters the MST, there is a vacuum beam dump. Keeping the beam dump under vacuum eliminates the need for a second vacuum-to-air interface, which could increase the background scattered light. The spectrometer and collection fiber optics are located in a light-tight cabinet at the top of a pair of nearly vertical support beams, which attach to the laser cart. In this way, the entire Thomson scattering laser system remains mechanically and electrically isolated from the MST.

The MST ruby-laser system can be operated in two configurations, which are related to the regions of plasma volume that are of interest for a particular experiment. The Thomson scattering volume that is viewable by the system is the image of the fiber optic bundle on the beam line. In the “central laser path” configuration, there are eight chords of measurement extending from $r/a = -0.587$ to $r/a = +0.627$. Here the negative sign refers to chords that are inboard of the geometrical center of the MST vacuum vessel. In the “edge laser path” configuration, a steering mirror is inserted into the beam line, directing the laser onto a more tangential path to the plasma. In “edge” configuration the radial locations that are measured cover a range from $r/a = 0.625$ to $r/a = 0.882$. Figure 2 gives an indication of the extent of the radial coverage.

III. LIGHT DETECTION SYSTEM

Thomson scattered photons are collected by a 3-in.-diam lens located in the box port flange. This light is focused onto a movable fiber optic bundle and piped into a Jarrell-Ash

Monospec-27 spectrometer. At the entrance to the fiber bundle are a cut-glass filter and a plastic polarizer that are used to reduce non-Thomson scattered, background light. The spectrometer entrance aperture is set by a 0.072 in. slot attached to the end of the fiber bundle. The spectrometer uses one of three gratings to disperse the incoming light.

The most recent upgrade to the Thomson scattering system replaced the five-channel microchannel plate (MCP) detector with an 11-channel large area-avalanche photodiode detector (LA-APD) array. To do this the exit-plane mirror of the spectrometer was removed and a new exit-plane structure was fabricated. This new exit-plane structure consists of two bundles of fiber optics, which are fastened to a kinematic mount. These two bundles contain seven (on the long-wavelength side) and four (on the short-wavelength side of the laser line) separate sub-bundles of fibers for dedicated LA-APD modules. Because the plastic fibers (1-mm-diam ESKA-MEGA) used to construct this array slightly attenuate the light at the frequencies of interest, it is necessary to minimize the distance between the exit-plane and the LA-APD detector element.

The LA-APD modules themselves are commercially available units from Advanced Photonix, Inc. The photodiode has a 5-mm-diam active area. The APD is thermoelectrically cooled to maintain a high signal-to-noise ratio (SNR). The improvement in the SNR is due to the high quantum efficiency of the LA-APD at the ruby wavelength compared to the MCP, about 85% vs 3.5%. The main advantage of the MCP was its relatively high gain, 10^6 , as compared to

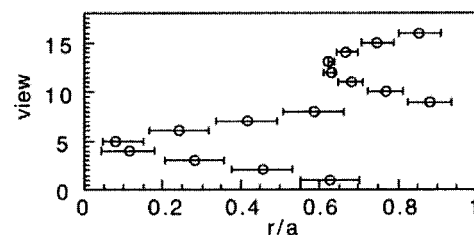


FIG. 2. Geometrical coverage of ruby-laser Thomson scattering views. Error bars indicate radial range (in r/a space) of scattering volume on each view.

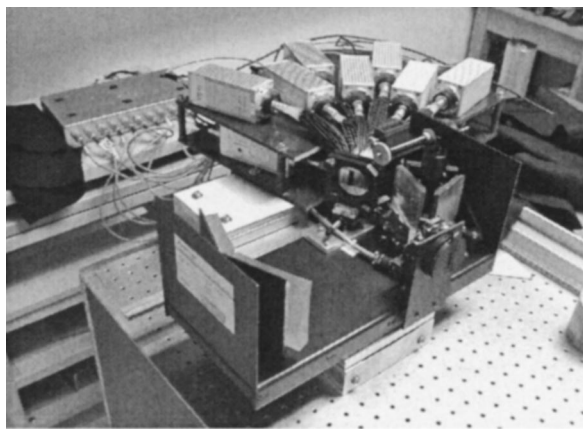


FIG. 3. Photograph of the TS spectrometer. The two-tier, stadium style layout of the LA-APD modules, the exit-plane fixture, the larger area mirror, the spectrometer shutter, and the APD power distribution box are visible.

the LA-APD gain of approximately 300.⁵ Another difference between the APD modules and the MCP is that the APDs have a continuous signal output, whereas the MCP could only be gated on for a few microseconds. Because the APDs are always “on,” it was necessary to install a fast-opening shutter in the spectrometer. This shutter remains closed during “start-up” of the plasma discharge to block out the intense background light. Measurement based calculations indicate that the plasma start-up light would exceed the manufacturer’s damage threshold of the APD by close to an order of magnitude. A photograph of the assembled spectrometer, exit plane, and LA-APD array and shutter can be seen in Fig. 3.

IV. ELECTRONICS AND DIGITIZATION

A schematic overview of the MST TS system is shown in Fig. 4. Working back from the data acquisition system, Thomson scattering data is digitized using either 3 LeCroy 2249A or 3 LeCroy 2250L digitization modules. The main difference between the two types is that the 2250L’s have 32 bit fast in fast out memory. This allows the modules to be re-triggered with a minimum separation time of 9 μ s. This feature is extremely important for double-pulse experiments, and is convenient when calibrating the system. Both types of modules integrate the charge delivered to their 12 parallel inputs for 100 ns, when the module is gated on. This gate width gives an adequate amount of flexibility for any jitter in the initial timing of the fast-photodiode triggering, which will be discussed below.

Three digitizers are used to capture: (1) the background light preceding the Thomson scattering signal, (2) the Thomson scattering signal, and (3) the background light following the Thomson scattering signal. To accomplish this the signals from the 11 LA-APD modules are triplicated using 11 0°, three-way power splitters, available commercially from Mini-Circuits, Inc. The sensitivity of these power splitters ranges from 10 kHz to 2 GHz. One drawback of this scheme is the loss of “dc” background light from the plasma. This represents a possible source of error, not in the temperature, but in the uncertainty of the number of photons. The temperature is unaffected, since subtracting the average of the two digitized background signals from the digitized TS signal removes this dc background. In addition to the filtering done by the power splitters, each APD signal is also filtered by an isolation transformer, used primarily to prevent internal ground loops. The iso transformers used are simple inte-

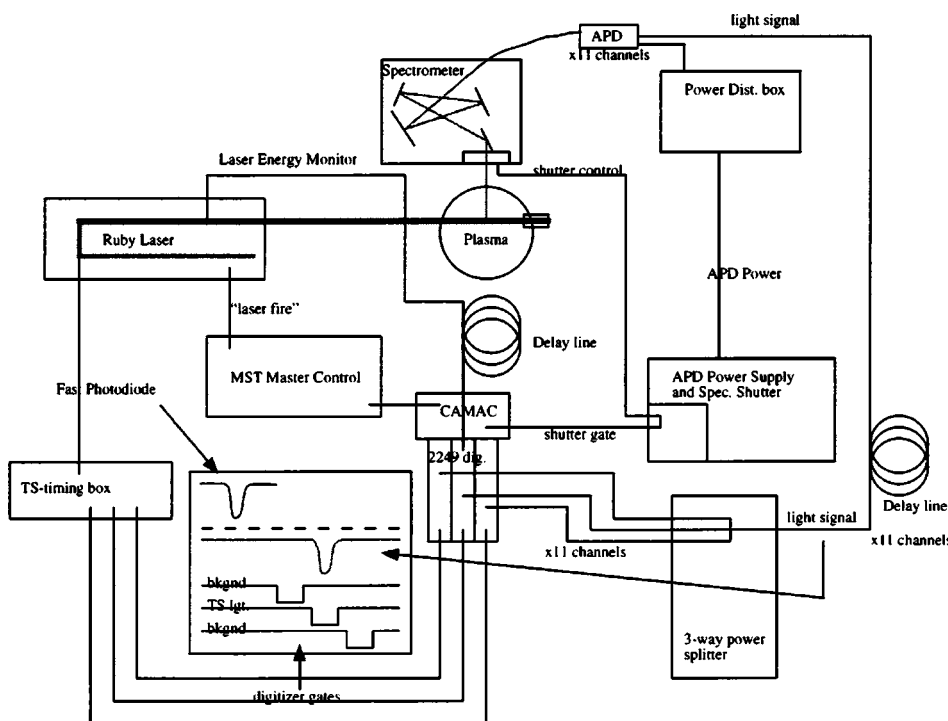


FIG. 4. Schematic overview of the ruby-laser TS system.

grated circuits (chip 8451-IP), which have a 3 ns rise time.

The timing of events in the MST Thomson scattering system is entirely controlled by the measurement of the laser fast-photodiode output. This photodiode detects a small fraction of the photons that are emitted by the oscillator ruby rod during lasing. From that point onward, the majority of the timing is set by the time-of-flight physical separation of objects and by lengths of delay line. A properly timed sequence of events is shown schematically in Fig. 4. The “laser fire” trigger can be adjusted to occur nearly anywhere within the plasma discharge. The laser fire signal may be given manually, or via the CAMAC based, MST timing circuitry. A mechanical shutter is used to block the intense burst of plasma start-up light at the beginning of the discharge, which could damage the detectors. The shutter has a finite opening time of 3 ms. After laser fire is given to the laser, roughly 1.25 ms are required for the flash lamps to fire and pump the ruby rods.

V. SUMMARY

This article has discussed in detail the hardware utilized in the MST ruby-laser Thomson scattering system. Though the ruby laser system has performed routinely on the MST, its single-point in space and time hindrances are beginning to limit the types of phenomena that can be studied. To address this limitation, a new multi-point, 100 Hz sampling rate, yttrium–aluminum–garnet laser system is being implemented on the MST for Thomson scattering measurements. This new system will in many ways render the old ruby system obsolete. However, in the meantime the ruby TS system remains the only way to make noninvasive measurements of T_e in the MST. Measurements made recently have shown the importance of relativistic considerations when examining temperatures greater than 1 keV.⁶ These measure-

ments were made possible by the increased spectral coverage of the upgraded ruby-laser TS system on the MST. The SNR improvement afforded by the LA-APD array also made it possible to study time resolved electron temperature profiles in the MST for the first time. The electron temperature evolution has been measured in a number of different discharge conditions.⁸ Under typical plasma conditions, these measurements have demonstrated the role of magnetic fluctuations in the transport of heat, and would not have been possible without this diagnostic upgrade.⁹

ACKNOWLEDGMENTS

The authors wish to recognize the many contributions of the UW-Madison MST group. This work was supported by the U.S. Department of Energy, in particular the Magnetic Fusion Science Fellowship program.

¹R. N. Dexter, D. W. Kerst, T. W. Lovell, S. C. Prager, and J. C. Sprott, *Fusion Technol.* **19**, 131 (1991).

²D. J. Den Hartog, Ph.D. thesis, University of Wisconsin-Madison, 1989.

³M. R. Stoneking and D. J. Den Hartog, *Rev. Sci. Instrum.* **68**, 914 (1997).

⁴M. Cekic, D. J. Den Hartog, G. Fiksel, S. A. Hokin, D. J. Holly, S. C. Prager, and C. Watts, presented at the American Physical Society's 34th Annual Meeting of the Division of Plasma Physics, Seattle, 1992 (unpublished).

⁵M. R. Stoneking, D. J. Den Hartog, M. Cekic, and T. Biewer, PLP Report No. 1181, University of Wisconsin-Madison, 1996.

⁶B. E. Chapman, A. F. Almagri, J. K. Anderson, T. M. Biewer, P. K. Chattopadhyay, C.-S. Chiang, D. Craig, D. J. Den Hartog, G. Fiksel, C. B. Forest, A. K. Hansen, D. Holly, N. E. Lanier, R. O'Connell, S. C. Prager, J. C. Reardon, J. S. Sarff, M. D. Wyman, D. L. Brower, W. X. Ding, Y. Jiang, S. D. Terry, P. Franz, L. Marrelli, and P. Martin, *Phys. Plasmas* **9**, 2061 (2002).

⁷D. J. Den Hartog and M. Cekic, *Meas. Sci. Technol.* **5**, 1115 (1994).

⁸T. M. Biewer, Ph.D. thesis, University of Wisconsin-Madison, 2002.

⁹T. M. Biewer, J. K. Anderson, G. Fiksel, B. Hudson, J. C. Wright, S. C. Prager, C. B. Forest, W. X. Ding, and S. D. Terry, *Phys. Rev. Lett.* (submitted).